This article has been accepted for inclusion in a future issue of this journal. Content is final as presented, with the exception of pagination.

Evaluation of Brightness Temperature Sensitivity to Snowpack Physical Properties Using Coupled Snow Physics and Microwave Radiative Transfer Models

Do Hyuk Kang, *Member, IEEE*, Shurun Tan, *Member, IEEE*, and Edward J. Kim, *Senior Member, IEEE*

***Abstract*— There are multiple existing microwave radiative transfer models (RTMs) to simulate the brightness temperature (Tb) of snowpacks. It is still challenging to have consistent Tb responses from RTMs due to individual physical formulations of the snowpack scattering process. This article examines three of the widely-used multi-layer RTMs: 1) the microwave emission model of layered snowpacks (MEMLS); 2) the dense media radiative transfer based on the quasi-crystalline approximation (QCA) of Mie scattering of densely packed sticky spheres (DMRT-QMS); and 3) the Helsinki University of Technology (HUT) model. Interestingly, these models yield slightly different Tb responses when driven by the same physical snowpack properties. Tb variations, dependent on the choice of RTMs, are then evaluated to improve the understanding of model differences in microwave emission from a snowpack. We first perform a sensitivity study of the Tb predictions from the three RTMs as a function of snow grain sizes, densities, and depths. While Tb from all three RTMs decreases with increasing snow grain sizes, it is found that a scaling factor is required to have the same amount of Tb attenuation for small grain sizes within the Rayleigh scattering regime. For larger grain sizes, however, a scaling coefficient is not enough to match the model outputs due to the different scattering assumptions of the RTMs. For a single snow layer with increasing snow depths and densities, all three RTMs exhibit Tb attenuations arising from the increase in path lengths and optical depths. Further evaluations are conducted by feeding the three RTMs with the output of a snow physics model driven by *in situ* weather forcing in a coupled simulation. Outputs of this coupled model include snowpack physical properties and Tbs. By using snow stratigraphy observations, another set of Tb simulation is also conducted with RTMs driven by *in situ* snowpit observations. The snow physics outputs from the coupled case are compared against *in situ* snow stratigraphy observations. And both Tb simulations are compared against ground-based microwave observations from the European Space Agency (ESA) Nordic Snow Radar Experiment (NoSREx) 2009–2012. For three consecutive years, the *in situ* driven Tbs have 21.0-K root-mean-squared error (RMSE) while the coupled simulations have 24.7-K RMSE. However, after isolating the dry snow period and excluding diurnal melting snow conditions, 12.2- and 6.3-K RMSEs are achieved from *in situ* and coupled cases, respectively, in the 2011 water year.**

***Index Terms*— Correlation length, dense media radiative transfer based on the quasi-crystalline approximation (QCA) of Mie scattering of densely packed sticky spheres (DMRT-QMS), grain size, Helsinki University of Technology (HUT), microwave emission model of layered snowpacks (MEMLS), Nordic Snow Radar Experiment (NoSREx), snow density.**

I. Introduction

IN MICROWAVE earth remote sensing retrieval algorithms that employ data assimilation (DA), radiative transfer models (RTMs) play an essential role [1]. In such DA retrieval frameworks, the RTM simulates microwave signals from earth and enhances the predictability of atmospheric profiles [2] and earth surface variables, such as vegetation [3] and terrestrial snow [4]. Retrieval algorithms for terrestrial snow using microwave remote sensing have been advanced significantly, since the pioneering launch of the scanning multichannel microwave radiometer (SMMR) [5]. For spaceborne observations, the microwave frequencies utilized are typically from 1 to 100 GHz, isolated in several frequency windows where the atmosphere is relatively transparent to microwave. At these frequencies, the brightness temperature (Tb) is an observable related to the amount of microwave emission from the snowpack. In general, the upward emission from soil is attenuated by the snow layers due to the scattering inside the snowpack while the emission from the snowpack contributes to the upward emission. Microwave scattering and absorption in the snowpack are controlled by the physical parameters of stratified snow, including the snow temperature, density, depth, grain size, and liquid water content in each layer [6]. To invert snowpack parameters from Tb observations at microwave frequencies, RTM forward simulations utilize a set of dielectric mixing and scattering models of the snowpack physical properties. Here, the dielectric mixing models [7] and the scattering behaviors of snow [8] are determined by the structure of ice particles, air, and liquid water in the snowpack.

Manuscript received November 16, 2018; revised April 3, 2019 and May 31, 2019; accepted July 29, 2019. This work was supported in part by the NASA Terrestrial Hydrology Program under Grant 80NSSC18K1136 and in part by the NASA Postdoctoral Program at the Goddard Space Flight Center, administered by Universities Space Research Association through a contract with NASA. *(Corresponding author: Do Hyuk Kang.)*

D. H. Kang is with the Earth System Sciences Interdisciplinary Center, University of Maryland, College Park, MD 20742 USA, and also with the NASA Goddard Space Flight Center, Greenbelt, MD 20771 USA (e-mail: dk.kang@nasa.gov).

S. Tan was with the Radiation Laboratory, Department of Electrical Engineering and Computer Science, University of Michigan, Ann Arbor, MI 48109 USA. He is now with the joint Zhejiang University/University of Illinois at Urbana–Champaign Institute, Haining 314400, China (e-mail: srtan@intl.zju.edu.cn).

E. J. Kim is with the Hydrologic Sciences Laboratory, NASA Goddard Space Flight Center, Greenbelt, MD 20771 USA (e-mail: ed.kim@nasa.gov).

Color versions of one or more of the figures in this article are available online at http://ieeexplore.ieee.org.

Digital Object Identifier 10.1109/TGRS.2019.2932732

0196-2892 © 2019 IEEE. Personal use is permitted, but republication/redistribution requires IEEE permission.
See http://www.ieee.org/publications_standards/publications/rights/index.html for more information.

This article has been accepted for inclusion in a future issue of this journal. Content is final as presented, with the exception of pagination.

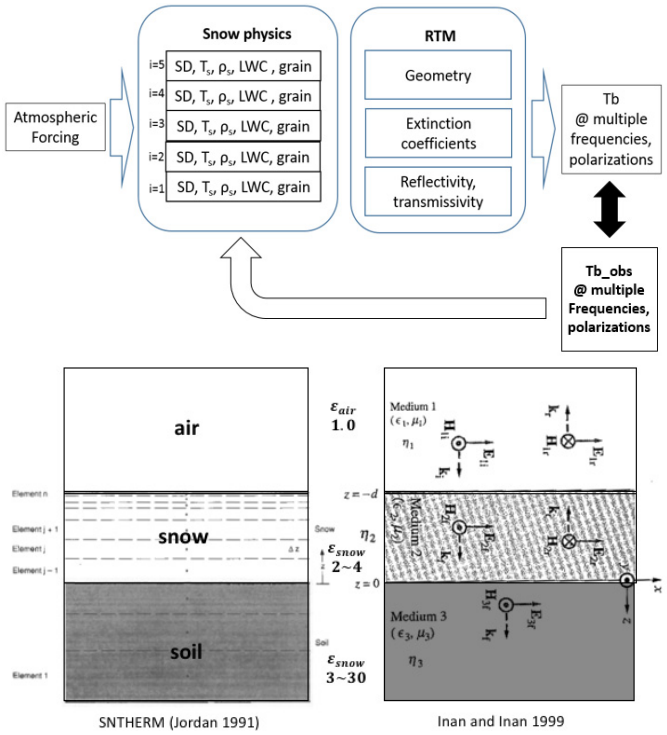


Fig. 1. (Top) Terrestrial snow retrieval by comparing Tb simulations against Tb observations. (Bottom) Schematic of air-snow-soil layers together with an illustration of microwave interaction with the layers [modified from 18 (Left) and 19 (Right)].

Thus, the choices of RTMs are one of the contributing factors to accurately simulate microwave signatures from a snowpack.

In this article, we consider two options of driving an RTM using snowpack profiles: 1) driven by the purely *in situ* snow stratigraphy and 2) driven by the snow profiles predicted by a snow physics model [10]. The snow physics model method requires a meteorological forcing data set with air temperature, precipitation, wind speed, relative humidity, and solar radiation at each time step. Using snowpack profiles as an input, the RTM then predicts the microwave Tb by solving radiative transfer equations to account for microwave interactions within the snowpack [10], [11]. The first option is useful for identifying error sources within the RTM while the second option has the potential to be applied in DA. A DA framework for retrieving snow parameters from passive microwave observations involves comparing simulated Tb and observed Tb and minimizing Tb differences using various statistical methods. The retrieval relies on the snow physical models to estimate the state variables of snowpacks. Fig. 1 (top) shows this retrieval approach [12].

This article focuses on the intercomparison of three RTMs, as shown in Fig. 1 (top): 1) the microwave emission model of layered snowpacks (MEMLS [12], [13]); 2) the dense media radiative transfer based on the quasi-crystalline approximation (QCA) of Mie scattering of densely packed sticky spheres (DMRT-QMS [14]); and 3) the Helsinki University of Technology (HUT [15]) model. The detailed descriptions of each RTM are in Section II-B. Tedesco and Kim [16] have conducted an intercomparison of four RTMs by using the single snow layer simulations. This article extends the RTM intercomparisons by using controlled sets of snow inputs and model-based RTM simulations applied to the actual snow data set, along with the single and multi-snow layer formulations.

In particular, Löwe and Picard (2015) [19] attempted to evaluate scattering coefficients of both MEMLS and DMRT-ML (an implementation of DMRT-QCA with coherent potential approximation). Assuming sticky hard snow spheres, they concluded that MEMLS-IBA (by using an improved-born approximation [13]) and DMRT-ML predict identical behaviors of scattering, and established a quantitative relationship between the grain radius of the sticky-hard-sphere (SHS in DMRT) and the correlation length in MEMLS to predict the similar scattering behavior. This analysis of scattering behaviors based on different RTMs is analogous to an implementation of a Fourier Transform of the correlation function in MEMLS [13] and an alternative calculation through QCA approximation in DMRT-QMS. Royer *et al.* [20] also examined DMRT-ML [19], [21], DMRT-QMS [14], HUT [15], and MEMLS [12], [13] to examine snow grain size scaling issues, and provided conversion rules for the grain sizes used in each model. The specific surface area (SSA) was recommended as a more objective quantity for snow grain size description, ready to be converted into specific snow grain variables for each RTM.

By considering the importance of snow microstructure with respect to microwave signatures, there have been many recent attempts to describe the impacts of snow grain size in RTMs. MEMLS and HUT model comparisons conducted by Pan *et al.* [22] showed overestimation of scattering coefficients in HUT. This overestimation leads to an underestimation of Tb for deep snow in HUT. Intensive validation experiments were performed, including Sodankylä Finland, Churchill Canada, and Colorado USA. The Nordic Snow Radar Experiment (NoSREx) data sets are used to validate the RTMs. Sandells *et al.* [23] conducted another comprehensive intercomparison of the three RTMs (HUT, MEMLS, and DMRT-QMS) within a consistent snow modeling framework. By comparing the compatibility between snow model microstructures and microwave emission models, the optimal scaling factors were determined. This article demonstrates it is essential to parameterize snow microstructures, which leads to improvement in microwave emission models.

This article not only extends the long-term efforts and methodologies for snow dielectric and scattering studies [6]–[8] but also tries to improve microwave forward model algorithms, and it therefore reports comprehensive results from both controlled and coupled simulations, which directly relate snow physical properties with the passive microwave signatures.

Both physical and electromagnetic representations of the air-snow-soil layers are conceptually shown in Fig. 1 (bottom). One objective of this article is: 1) to find a suitable treatment of forward modeling parameters by evaluating differences in existing RTMs driven by gradually changing snow physical properties. This article first conducts several controlled RTM-only experiments to compare the Tb responses of the

This article has been accepted for inclusion in a future issue of this journal. Content is final as presented, with the exception of pagination.

three RTMs to gradual changes in snow physical parameters, such as the snow grain size, snow density, and snow depth, which are the main drivers of snow physical properties regardless of RTMs; 2) to determine what dominates Tb from the snow physics model driven by a weather forcing data set; and 3) to quantify Tb uncertainties associated with temporal changes of the snow water equivalent (SWE) during the entire water year. To achieve the second and third goals, coupled and *in situ* driven Tb simulations are conducted based on meteorological forcing data sets and ground-truth snowpit observations from NoSREx. Both Tb simulations are compared against the ground-based microwave observations at NoSREx to evaluate Tb uncertainties during the evolution of the SWE.

This article is organized as follows. Section II first addresses a summary of critical issues in the role of snow microstructure toward microwave observations, then describes three RTMs in detail, and the setup of Tb sensitivity tests and coupled evaluations. Section II also includes the description of the validation data sets extracted from NoSREx, such as the meteorological forcing data set, and *in situ* snowpit measurements. Results from the controlled experiments of all three RTMs are described in Section III. Section IV demonstrates a set of realistic simulations of snowpacks and associated Tbs conducted by coupling each RTM with the multi-layered snow physics model and with *in situ* snow stratigraphy observations. The snow physics model is here driven by the observed atmospheric forcing, and the results are validated against NoSREx Tb observations. Finally, summaries and recommendations are presented in Section V regarding the RTMs both in the controlled and the coupled/*in situ* driven Tb simulations.

II. Methodologies

A. Snow Microstructure: Coupling Snow Physics Model With RTMs

Snow grain size has been identified as the most critical microstructure parameter related to microwave forward modeling. However, each RTM uses different methods to represent snow grain sizes. In MEMLS, snow is treated as a random media, and a two-point correlation function is chosen to characterize the two-component random media, ice and air. In practice, the two-point correlation function is characterized by a correlation length, p_c. HUT, being more empirical, defines an "equivalent grain size" of the snowpack that is either related to the "visual grain size" ($D_{\max}$) or the "optical grain size" (D_o) through regression training. The physical model of QCA, as adopted in DMRT-QMS, is a discrete scattering model that utilizes SHSs to represent the ice grains in the snowpack. An SHS is defined by two parameters: a grain diameter, D_g and a stickiness parameter, τ_g. D_g is also a length-scale equivalent parameter, and it is typically perceived that $D_o < D_g < D_{\max}$. τ_g on the other hand, characterizes the tendency of individual grains aggregating to form clusters.

Field observation techniques to characterize snow microstructure have significantly advanced over the years. The original eyeball estimation of $D_{\max}$ against a gridded board approach has been replaced by more objective and rigorous measurement of the SSA, which directly relates to the optical grain size (D_o). Micro-computer X-ray tomography (micro-CT) can also be applied to obtain the microstructure of snowpack directly, from which the correlation function can be readily derived. Even with technological advances, it is still challenging to quantitatively apply the snow grain size into a microwave RTM framework.

With an effort to intercompare these individual snow grain parameters in an RTM, Mätzler [24] comprehensively summarizes the relationship among p_c, D_{effc}, and D_o. By assuming a spherical grain size type, we choose to use D_{effc} instead of $D_{\max}$ (equal to D_{eff}), and D_o (here, equal to D_{effc}). The correlation length, p_c for MEMLS can be calculated from D_o by using Montpetit *et al.* [25] and Mätzler [24]

$$p_c = 2/3 \cdot (\rho_s/\rho_{\text{water}}) \cdot D_o \tag{1}$$

where ρ_s and ρ_{water} are snow and water densities in g/cm^3, respectively, and p_c is the correlation length in mm.

On the other hand, despite substantial efforts in developing microwave forward models for snowpacks, choosing an RTM for terrestrial snow remote sensing requires special care. Changes in snow physical variables such as the snow grain size, density, and depth all lead to Tb variations. Retrievals of one parameter are thus strongly dependent on the accurate estimation of other critical parameters.

Durand *et al.* [26] address the sensitivities of changes in critical snow parameters inverted from passive microwave snow remote sensing observations. With prior estimates of snowpack properties simulated by a land surface model, the snow depth bias is shown to decrease from -53 to -7.3 cm. To reduce the large uncertainties associated with changes in snowpack physical properties, Wiesmann *et al.* [27] introduced the idea of coupling the snow physics model with an RTM; and Langlois *et al.* [9], Wiesmann *et al*. [27], and Kang and Barros [28] also demonstrated coupled model results. The potential to use a coupled model as a remote sensing forward operator can thus be explored by dynamically relating the microwave radiometric properties to snow physical properties. Kontu *et al.* [29] also addressed a coupled snow hydrology model with HUT to evaluate the effects of modeled grain size parameters on passive microwave behaviors of the snowpack.

B. Three RTMs: MEMLS, HUT, and DMRT-QMS

MEMLS [12], [13] was developed to simulate Tb from a multi-layered snowpack. Using six-flux theory, MEMLS considers multiple scattering and absorption, including radiation trapping due to internal total reflections and combinations of coherent and incoherent reflections between layer interfaces. MEMLS initially determines scattering coefficients empirically, and then the IBA was adopted to determine scattering coefficients for large snow grain sizes [13].

The HUT snow emission model is a radiative transfer-based semiempirical model of snowpack emission that assumes a multi-layered snowpack. Each layer of the snowpack is characterized by the depth, temperature, effective grain size, and density of snow. The HUT was initially developed assuming a single snow layer, before the Finnish

This article has been accepted for inclusion in a future issue of this journal. Content is final as presented, with the exception of pagination.

Meteorological Institute (FMI) adapted it for multi-layer snowpacks [15], [29], [30]. The impedance of each layer and the boundary reflectivities are used to solve for the microwave intensity within each snow layer. In addition to the snowpack itself, forest and mixed-scene corrections are included in the HUT model, and thus, it allows comparing simulated Tb with Tb observations from airborne or satellite microwave sensors.

DMRT-QMS is a physical model, based on analytically solving multiple scattering among densely packed sticky spheres using the quasi-crystalline approximation (QCA). It provides a wide range of frequency and size dependences of the scattering coefficients, and predicts moderate forward scattering patterns, depending on the physical parameters of the snowpack. Such a physical approach is valid over a wider range of regimes than empirical models. DMRT-QMS has undergone over 15 years of development and tests since Tsang *et al.* [14] to represent the microwave scattering behavior of random media such as snow. In DMRT-QMS, the radiative transfer equation is solved using the discrete coordinate method with eigenvalue analysis. It considers detailed scattering patterns and includes multiple scattering among particles and multiple reflections among layers. Specifically, DMRT-QMS has a robust treatment of microwave scattering behavior. The phase matrix is used to couple the scattering from one incidence direction to all the scattering directions, and it is controlled by the grain size, the stickiness parameter, and the ice volume fraction of snow. The DMRT-QMS predicts both Tbs and backscattering coefficients from the snowpack and; therefore, it is applicable to both active and passive microwave snow remote sensing. Combined active and passive observations are expected to reduce ambiguities in SWE retrievals.

C. Two Experimental Setups: Controlled Versus Realistic

We describe two types of experiments: "controlled" and "realistic." The controlled experiments are designed to evaluate different Tb responses as a function of the three main parameters: snow grain size, density, and depth. With other snow inputs held constant, the effects of each of these three parameters were systematically examined. For the realistic experiments, a snow physics model forced by weather provides inputs for RTM simulations. Thus, these two experiment setups are aimed at evaluating the sensitivity of RTMs to snowpack physical properties.

Table I summarizes the snow inputs used in the three RTMs. HUT and DMRT-QMS represent the underlying soil beneath the snowpack with soil relative permittivity and roughness while MEMLS does not consider the effect of the soil boundary. A coupled simulation is achieved by relating the three RTMs to a snow physics model. One of the unique elements of the coupled experiments is to provide direct comparisons of simulated and observed Tbs. The Tb outputs from the three RTMs are compared against the *SodRad*, ground-based radiometer measurements deployed in NoSREx. This coupled model practice is therefore useful to identify snow physics parameters most critical to Tb simulations, which are dynamically and individually driven by weather forcing data set.

TABLE I
SNOWPACK PHYSICAL PROPERTIES TO DRIVE MEMLS, HUT, AND DMRT-QMS

	MEMLS	**HUT**	**DMRT-QMS**
Layer Temperature	[K]	[°C]	[K]
Liquid Water Content	volume fraction	volume in percent	N/A (dry snow) but now updated with new implementation
Density	[kg/m^3]	[g/cm^3]	[g/cm^3]
Depth	[cm]	[mm] for SWE using Density and Depth	[cm]
Snow Grain Size	Corr. Length, p_c [mm], $p_c = 2/3 \cdot (\rho_s/\rho_{water}) \cdot D_o$	Effective Grain Size, D_{effc} [mm], $D_{effc} = 1.5 \cdot (1-\exp(-1.5 \cdot D_{max}$ or $D_o)$ [30, 32]	Optical Grain Size D_g [cm] and Stickiness Parameter,

Again, the realistic Tb simulation is also driven by *in situ* snowpit measurements from NoSREx.

D. Field Campaign Data Set: Nordic Snow Radar Experiment 2009–2012

The following description of NoSREx is extracted from the European Space Agency (ESA) report [32] and included here for completeness. Sponsored by ESA for the remote sensing retrieval of terrestrial snow, the NoSREx is undertaken to evaluate passive and active microwave observations on a large range of snowpack conditions in Sodankylä, Finland. The project is ultimately aimed at a future remote sensing mission observing terrestrial snow and ice to quantify cold region hydrological processes. A series of efforts were conducted as a part of Phase A studies for the ESA cold regions hydrology high-resolution observatory (CoReH2O), a dual-frequency synthetic aperture radar (SAR) satellite mission concept. The intensive observation area (IOA) hosted three ground-based microwave sensors including *SnowScat*, *Elbara-II*, and *SodRad*. *SnowScat* is a frequency scanning scatterometer operating from X-band to Ku-band (10.2, 13.3, and 16.7GHz); *Elbara-II* is a radiometer operating at L-band (1.4 GHz); *SodRad* is another radiometer operating from X-band through W-band (10.65, 18.7, 36.5, and 90 GHz). In the same location, *in situ* snow stratigraphy and soil samplings were coincidently and extensively conducted including manual snowpits at the Sodankylä site and snow surveys in a larger area, plus traditional automated snowpack sensors and

This article has been accepted for inclusion in a future issue of this journal. Content is final as presented, with the exception of pagination.

ground/classical meteorological observations. The campaigns also evaluated diurnal cycles in snow microwave properties, snow microstructure, grain size, and stratigraphy.

III. Controlled RTM Experiments

The Tb results are reported in this section only at 36.5 GHz. For the controlled RTM experiments, a single layer snowpack is assumed for the simplicity of the snowpack representations. Then, the Tb results are intercompared among the three RTMs. Only one of the three snow parameters, snow grain size, density, and depth are varied with all other snow inputs held constant. Below is the summary of the controlled experiment results for varying grain size, density, and depth, respectively.

A. Tb as a Function of Snow Grain Size

In our simulation of the Tb variation versus snow grain size, we choose the optical grain size D_o and/or D_{effc} assuming it is equal to D_o, as a representation of the snow grain size, and applied three scaling factors, α, β, and γ, relating to the grain size characterizations in MEMLS, HUT, and DMRT-QMS, respectively: for MEMLS, $p_c = \alpha p_c^0$, where $p_c^0 = (2/3)(1-(\rho_s/\rho_{\text{ice}}))D_o$ is from Pan [22] relation to link the correlation length with the optical grain size; for HUT, $D_{\max} = \beta D_o$; and for DMRT-QMS, $D_g = \gamma D_o$, while we fix the stickiness parameter $\tau_g = 0.1$ so that we only vary one parameter D_g to control the microstructure. We choose these scaling factors such that the three RTMs predict similar Tb attenuations for small grain sizes less than 1 mm when absorption and Rayleigh scattering dominate. The adopted values are $\alpha = 1.8$, $\beta = 1.0$, and $\gamma = 0.4$ to fit the same Tb values of three RTMs until 1-mm snow grain size. This lays the basis for further intercomparisons, and these values are kept unchanged both for the controlled and coupled RTM simulations throughout this study.

In Fig. 2, the Tbs are plotted as a function of D_{effc}, and the results are intercompared among MEMLS, HUT, and DMRT-QMS. The single snow layer has a 30 cm depth, 250 kg/m^3 density, and 263-K physical temperature. The ground underlying the snowpack has a physical temperature of 273 K, and a relative permittivity of $6 + i$. The observation angle is 53.1°. Tbs in general decrease with D_{effc}, and all three models predict very close Tb responses at the lower end of snow grain size for $D_{\text{effc}} \leq 1$ mm (the Rayleigh scattering zone). For the smallest grain sizes close to zero, the wave interaction inside the snowpack is governed by absorption rather than scattering.

This similarity in Tb responses reflects the fact that the three RTMs represent very similar absorption responses. For larger grain sizes beyond the Rayleigh scattering zone, however, the Tbs diverge: HUT overestimates Tb when the snow grain size increases. Such results are consistent with the fact that HUT assumes a square size dependence of extinction coefficient while MEMLS-IBA takes a close to cubic size dependence following the Rayleigh scattering assumption, and DMRT-QMS is purely physical and capable to predict the size and frequency dependences that fall in between that of HUT and MEMLS. Moreover, the DMRT-QMS model predicts scattering patterns that vary with frequency, stickiness, and

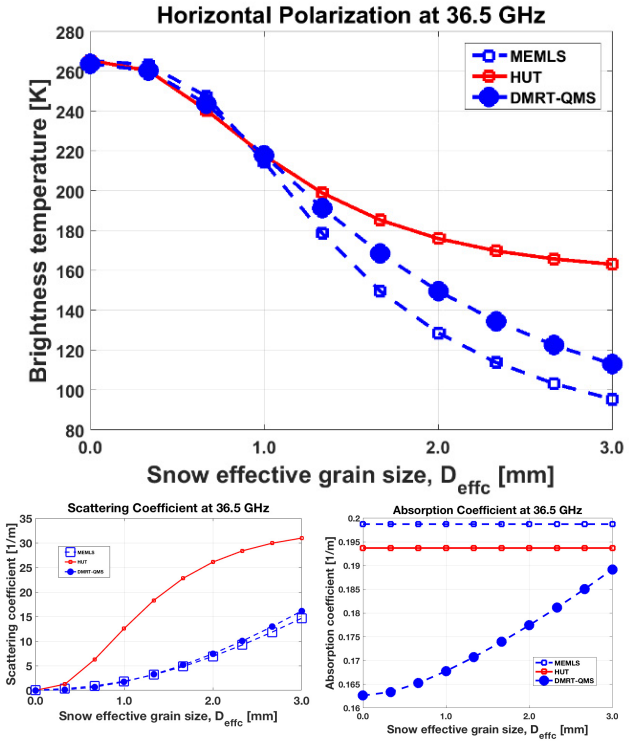


Fig. 2. (Top) H-pol. TB responses at 36.5 GHz, evaluated by MEMLS, HUT, and DMRT-QMS with increasing snow effective grain sizes. Fixed parameters: snow temperature = 263 K, snow effective grain size = 0.0–3.0 mm, snow depth = 30 cm, density = 200.0 kg/m^3, ground relative permittivity = $6 - i$ only for HUT, ground temperature = 273 K, and the incidence angle = 53.1°. (Bottom) Corresponding scattering and absorptions coefficients.

grain sizes. On the other hand, HUT assumes 96% forward scattering and ignoring the remaining 4% scattered power; MEMLS assumes close to the Rayleigh dipole scattering pattern despite adopting the IBA. A plot for the scattering coefficient supports the Tb underestimation of HUT compared to MEMLS and DMRT-QMS when increasing snow effective grain sizes.

B. Tb as a Function of Snow Density

Fig. 3 shows the Tb responses of the three RTMs as the snow density changes from 100 to 400 kg/m^3. The snow depth is a constant 60 cm (twice as deep as for the sensitivity test of grain size.). Fig. 3 shows that more extinction occurs as snow density increases. A slight drop of Tb from DMRT-QMS at 150 kg/m^3 can be explained by its nonconventional scattering behavior versus increasing snow density. Overall, DMRT-QMS also exhibits the Tb attenuation versus higher density. Compared to the changes in grain size, the absorption coefficient is more dominant to Tb responses in the case of changes in snow density.

C. Tb as a Function of Snow Depth

As snow depth increases (here, 1-mm snow grain size used), Tbs from all three RTMs display a monotonic decrease, with DMRT-QMS and HUT Tbs following each other closely, as shown in Fig. 4. These Tb decreases can be explained by

This article has been accepted for inclusion in a future issue of this journal. Content is final as presented, with the exception of pagination.

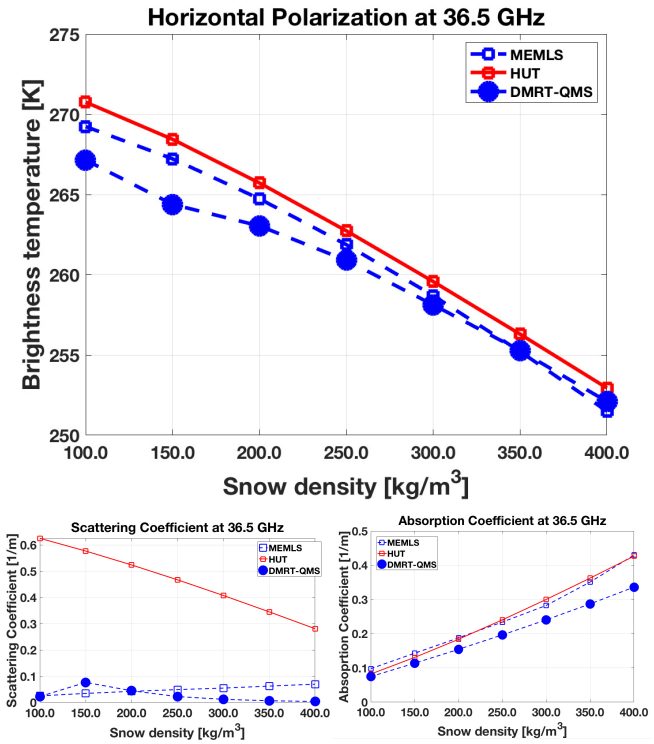


Fig. 3. (Top) H-pol. Tb responses with increasing snow density at 36.5 GHz, evaluated by MEMLS, HUT, and DMRT-QMS. Fixed parameters: snow effective grain size, $D_{\text{effc}} = 0.25$ mm, density = 100.0–400.0 kg/m^3, ground relative permittivity $= 6 - i$ (only for HUT), ground temperature = 263 K, snow depth = 60 cm, and the incidence angle = 53.1°. (Bottom) Corresponding scattering and absorptions coefficients.

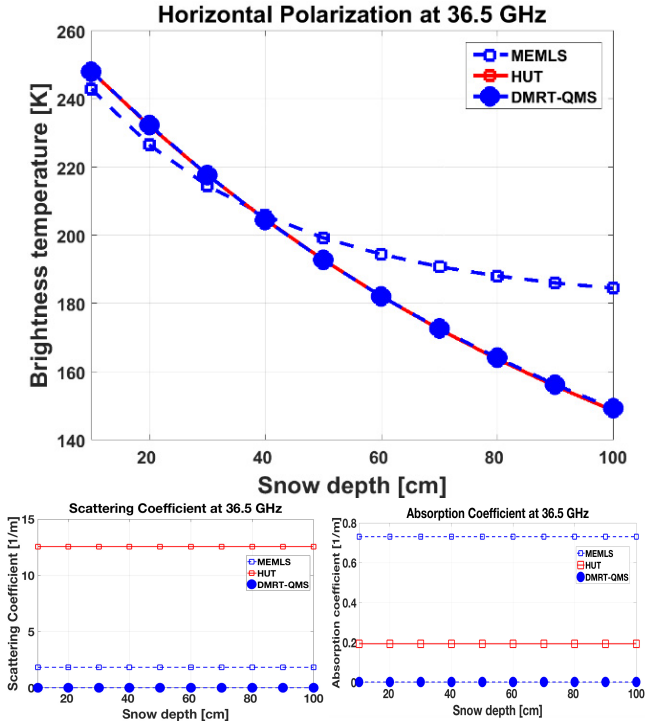


Fig. 4. (Top) H-pol. Tb responses with increasing snow depth at 36.5 GHz, evaluated by MEMLS, HUT, and DMRT-QMS. Fixed parameters: effective snow grain size, $D_{\text{effc}} = 1.0$ mm, density = 200.0 kg/m^3, ground relative permittivity $= 6 - i$ (only for HUT), ground temperature = 263 K, and the incidence angle = 53.1°. (Bottom) Corresponding scattering and absorptions coefficients.

a monotonic increase of the optical thickness as the snow depth increases. Here, the decay rate associated with the snow depth can be obtained from the coefficients of "$\exp(-\gamma \cdot SD_{\text{eff}})$," "$\exp(-(k_e - q2_{\text{mod}} \cdot k_s))$," and "$\exp(-\gamma \cdot \text{SD})$" for MEMLS, HUT, and DMRT-QMS, respectively. While Tbs are almost the same for HUT and DMRT-QMS, the optical thickness is underestimated in HUT compared to DMRT-QMS, so that the HUT Tb is higher. This is because the value of q_mod in $\gamma_s(1\text{-}q\text{_mod})$ in HUT's loss term is fixed at 96%. MEMLS Tb also shows a decreasing rate of change in Tb attenuation when approaching larger snow depths. Because the layer transmissivity, t decreases with snow depth, the layer emissivity, e increases, by conserving the energy associated, i.e., $e+r+t = 1$. Interestingly, the layer reflectivity r, is almost constant regardless of the snow depth, because $r = 1\text{–}e\text{-}t$ is very close to a single-scattering albedo definition, which shows that r is independent of the snow depth. This results in the slightly higher Tb in MEMLS, for larger snow depths. Constant values for the scattering and absorption coefficients are found along with the increase in the snow depth.

IV. Coupled and in Situ Driven Model Simulations Using NoSREx Data Set

This section covers RTM simulations coupled with a snow physics model driven by weather forcing. Here, the model is adopted from [28], and further implementations to handle an evolution of the snow grain size are included based on [33]. The column-based snow physics model receives weather forcing data set to accumulate a snowpack from the beginning, divides the snowpack into multi layers, and eventually melts when the air temperature goes above the melting point. The micro-structure such as the grain size is partially adopted from [33]. The weather data from NoSREx was used to drive all three RTMs simultaneously to produce Tb based on simulated snowpack physical conditions at each time step. The three Tb simulations are compared with the tower-mounted microwave observations, i.e., the ground-based remote sensing data set from NoSREx, observed by the microwave radiometer called *SodRad*. The outputs from the snow physics model are also compared to the *in situ* snowpit observations, in the IOA of NoSREx in Sodankylä, Finland during Water Years in 2010, 2011, and 2012. Another Tb simulation is made by driving the RTM (HUT) with *in situ* snowpit observations, thus forming two sets of Tb simulations, respectively, from the coupled and *in situ* driven cases.

A. Performance of the Snow Physics Model in the Coupled Case

Fig. 5 shows a three year-overview of snow depth simulations contrasted against the collocated snowpit observations. The snowpack model outcomes show good prediction performance, properly capturing the evolution of the snowpack compared against the ground-truth observations of the snow depth. Both modeled and observed snow start to accumulate in

This article has been accepted for inclusion in a future issue of this journal. Content is final as presented, with the exception of pagination.

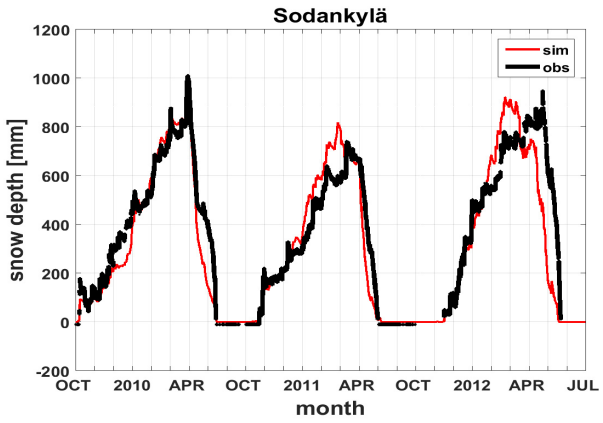


Fig. 5. Simulated snow depth validated against the observed snow depth from October 2009 to September 2012 from NoSREx in Sodankylä, Finland.

November and reach maximum depth in late March. Snowmelt occurs more rapidly than accumulation, potentially resulting in high snowmelt-runoff in April and May. In general, the snow depth simulation has demonstrated the robustness of the snow physics model in the coupled study.

Another advantage of running the snow physics model in the coupled case is that snow grain size, an essential input for certain RTMs, is also simulated. In the snow physics model, the grain size is primarily controlled by: 1) an initial size from snowfall and 2) a growth rate thermodynamically governed by snowpack temperature. The snow grain evolution in this application adopts the SNOWPACK model from Lehning *et al.* [33]

$$D_{\mathrm{effc}_{t+1}} = D_{\mathrm{effc}_t} + \Delta t \cdot D'_{\mathrm{effc}_t} \tag{2}$$

where

$$D'_{\mathrm{effc}_t} = C_1 \cdot sp \cdot \left(A_1 + \frac{A_2}{D_{\mathrm{effc}t}}\right) \exp\left(A_3 \left(\frac{1}{273.15} - \frac{1}{T_s}\right)\right). \tag{3}$$

D_{effc} is updated with a time step multiplied by the growth rate defined above where sp the is sphericity (equal to 1), $A_1 = 5.9 \times 10^{12}$, $A_2 = 9.4 \times 10^{-17}$, $A_3 = 2.9 \times 10^3$, and T_s is the snow temperature. Here, C_1 is defined by an adjustment factor to fit modeled Tb with observations. In addition to the equilibrium grain growth metamorphism implemented in (3), a kinetic growth rate described in [33] is also considered in this application of the snow physics model by using differences of each snow layer's temperature. Because D'_{effc_t} is defined by a rational function in (3), D_{effc} itself follows a natural log (ln) function shape with time owing to the integration of the rational function. Thus, D_{effc} slowly increases in the beginning, but the grain growth rate asymptotically decreases to form a logarithmic function. Again, D_{effc_i} and D'_{effc_t} are two parameters to describe changes in grain growth rates. For each Water Year, Table II displays D_{effc_i} and D'_{effc_t}.

Water year 2011 shows higher D_{effc_i} compared to the water year 2010 and 2012. D'_{effc_t} is also highest in the water year 2011, indicating a steeper increase of D_{effc}. It appears that the relationship between Tb and the behavior of the observed optical grain size is captured well on an annual basis. It follows that implementations of the snow grain size are essential for RTM simulations for Tb.

TABLE II

ANNUAL INITIAL EFFECTIVE SNOW GRAIN SIZES, THEIR GRAIN GROWTH RATES, AND THE ADJUSTMENT FACTORS BASED ON SIMULATIONS

Water Year	D_{effc_i} [mm]	$D_{effc_t}{}'$ [mm/day]	C_1
2010	1.2	0.0014	1.0
2011	1.5	0.0035	2.5
2012	1.0	0.0005	0.4

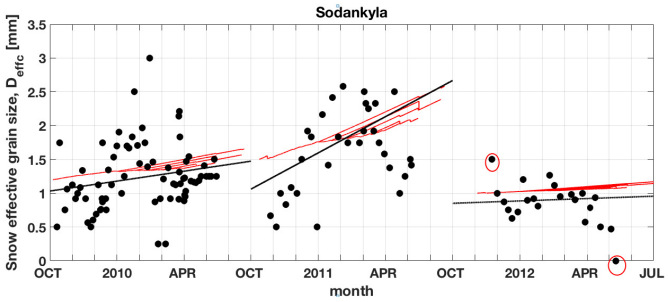


Fig. 6. Simulated multi-layered snow grain size evolution with red lines compared against the IOA snowpit observation (temporally averaged at each snowpit sampling) for water years 2010, 2011, and 2012. Linear lines are based on the *in situ* snowpit observations.

Fig. 6 shows the simulated multi-layered snow grain size to the *in situ* grain observations from the IOA in NoSREx. The number of snow layers increases from a single layer to 5∼6 layers, as snow accumulates. Please note that observed snowpit observations are vertically averaged at each point of snow extraction. Thus, D_{effc} also has a multi-layer character (vertically averaged at each snowpit), as shown in Fig. 6. The observed snow grain size exhibits wide scatter. Each water year has a linear line from *in situ* snow grain size observations, which represent the grain growth rates associated with the ground measurements. The first and third water years well represent the *in situ* observations from the snow physics simulations. It is noted that the second year is only represented with the bottom two layers from the *in situ* observations. The second year indicates more influence from the bottom layers (above 2 mm of coarse grain size) is identified with the proper Tb simulation to meet *SodRad* Tb observations. This can be explained by the fact that the snow depth is under 800 mm for the second year compared to the first and third year. This also indicates a deeper penetration depth of 36.5 GHz in the second year than the first and third years due to the shallow snow depth. In the third year, two outliers are excluded with the red circles. However, the simulations capture the increasing trend of the observed average grain sizes. Such increasing grain sizes are accompanied by the decreasing Tbs shown in Fig. 7.

Fig. 7 shows comparisons between the multi-layered snow density simulations and snowpit observations. Observed snow densities are averaged with all of the layers for a snowpit to

This article has been accepted for inclusion in a future issue of this journal. Content is final as presented, with the exception of pagination.

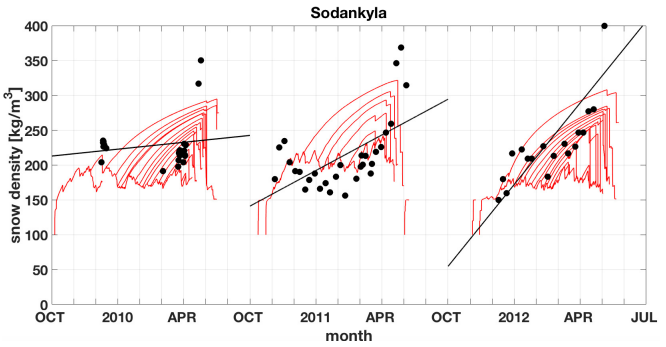


Fig. 7. Simulated multi-layered snow density with red lines compared against the IOA snowpit observation (temporally averaged at each snowpit sampling) for water years 2010, 2011, and 2012. Linear lines of the *in situ* observations are indicated.

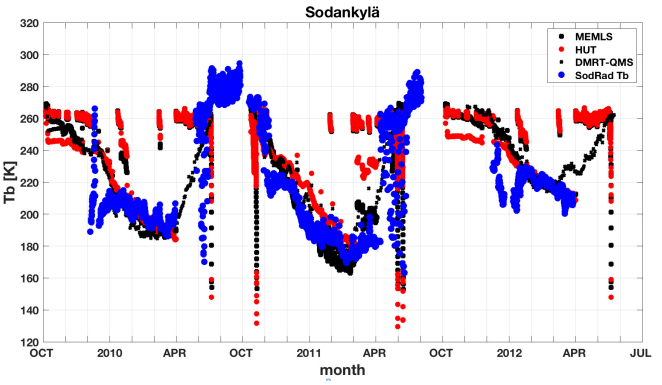


Fig. 8. Simulated Tbs driven by snow physics model outputs at 36.5-GHz h-pol. from three RTMs, MEMLS, HUT, and DMRT-QMS, compared against the *SodRad* Tb observations for water years 2010, 2011, and 2012.

provide one density value at a time. Similar to Fig. 6, the linear lines are embedded with the *in situ* observed snow density. The annual densities from both observations and simulations are varied from below 100 to almost 400 kg/m^3, with a 70% correlation coefficient between them. The model underestimates snow density when the snowpack reaches a density peak of 400 kg/m^3. This might be due to under-estimations of the liquid water in the snow physics model.

B. Coupling the RTMs With the Snow Physics Model

Fig. 8 shows Tb simulations from the three RTMs driven by outputs from the snow physics model. Tb observations from *SodRad* at NoSREx cover a duration from October 31, 2009 to July 30, 2012 spanning three water years. In general, Tb peaks observed by *SodRad* are likewise captured by all three RTMs. The early peaks are attributed to the presence of liquid water when snowmelt events occur in December. The increasing liquid water content in the snowpack increases the absorption coefficient so that emission (e) from the snowpack increases during melt events.

Melt-refreeze events often occur and form ice layers/lenses, resulting in a reduction of Tb. These multi-refreeze events are seen in model simulations during the early snow season in October, and also observed by *SodRad*. Overall, decreasing Tb trends at 36.5 GHz associated with snow accumulation are well captured in all three water years. However, average Tb

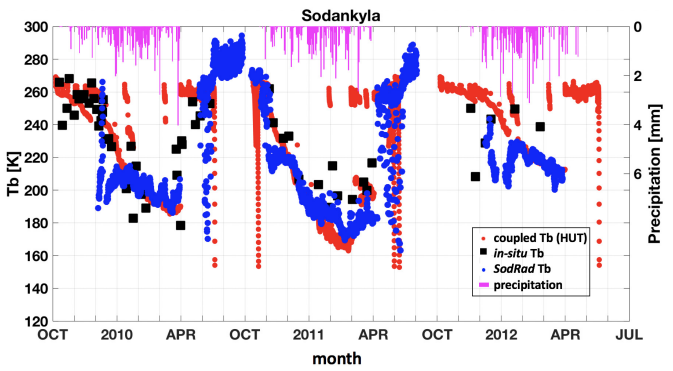


Fig. 9. Coupled model Tb, *in situ* snowpack-driven Tb, and *SodRad* observed Tb along with daily winter precipitation for water years 2010, 2011, and 2012. The HUT RTM is adopted in the Tb simulations.

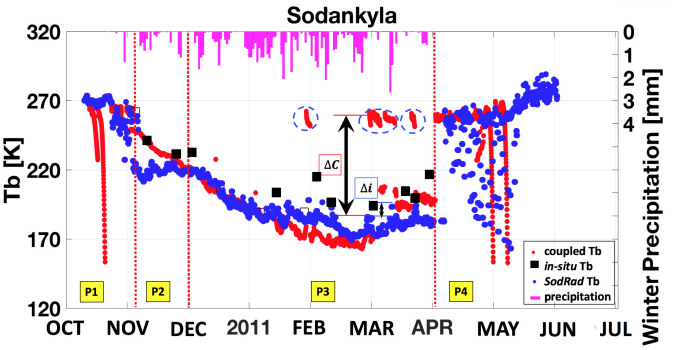


Fig. 10. Comparison between Tb simulations both with coupled and *in situ* driven against *SodRad* Tb observations in the water year 2011 along with winter precipitation. The water year 2011 is divided into periods P1∼P4.

attenuation is stronger in the water year 2011, and the highest Tb is present in water year 2012.

Fig. 9 shows: 1) the coupled Tb (HUT); 2) Tb driven by *in situ* snowpit against; and 3) *SodRad* observations. Both simulated Tbs 1) and 2) display attenuated behaviors due to scattering. The comparison is done with a moving average within 3 h to pair the coupled Tb with *in situ* driven Tb. A root-mean-squared error (RMSE) for *in situ* driven Tb is 21.0 K possibly due to effects of ice lenses on Tb [25, Montpetit *et al.*, 2013, 20.5-K RMSE], and the coupled case Tb RMSE is 24.7 K for all three water years. A difference of 3.7-K RMSE between *in situ* driven and coupled Tbs indicates uncertainties associated with a snow model within the coupled case. The larger RMSE in the coupled case is due to significant discrepancies arising from snow-melt at the start of the accumulation and melt seasons. In particular, Tb is highly sensitive to the liquid water content, but the timing of the presence of liquid water can be different between model simulation and observation. Even a few hours difference in the timing of the melt can make comparison statistics worse. The coupled case Tb exhibits more continuous Tb behavior (hourly time step) compared with *SodRad* (3-h time step), the agreement is best during the dry snow periods. In addition, several gaps of no-observation exist including April 2011 and after April 2012, thus making comparison statics worse.

Fig. 10 shows a close look between Tb simulations and observations in the water year 2011. Here, we note that the coupled Tb simulation is tuned to fit *SodRad* observations by adjusting the snow grain sizes described in Fig. 6. Also,

This article has been accepted for inclusion in a future issue of this journal. Content is final as presented, with the exception of pagination.

TABLE III

COMPARISON STATISTICS OF RMSE IN KELVINS FOR RTM SIMULATIONS DRIVEN BY *in situ* AND COUPLED METHODS BOTH AGAINST *SodRad* TB OBSERVATIONS ALONG WITH THE NUMBER OF COMPARISON PAIRS IN THE PARENTHESES

RMSE (K)	P1 (1)	P2 (3)	P3 (5)	P4 (1)
in-situ	5.6	11.9	**12.2**	33.7
coupled	13.9	15.2	25.9 **(6.3)**	37.9

the grain size scaling factors, $\alpha = 1.8$, $\beta = 1.0$, and $\gamma = 0.4$ are applied to both the coupled and *in situ* driven Tb simulations. This explains the better Tb match of the *in situ* Tb simulations than the coupled case Tb, as shown in Table III. Section IV-C describes the sensitivity of Tb to snow grain size in the coupled simulations.

For the water year 2011, the entire snow year is divided into four temporal periods: P1 through P4. RMSE calculations for each period are shown in Table III with respect to *in situ* and coupled simulations against *SodRad* Tb observations. During stage P1, defined as "the initial accumulation period," *SodRad* displays a decrease of Tb from 270 to about 230 K. The coupled simulation has an RMSE of 13.9 K for this period. This large RMSE is attributed to snowmelt in a single layer of the coupled model as seen by the two large Tb changes in mid-October. The large attenuation of Tb in the coupled case is also due to overestimation of the reflectivity in a thin snow layer because the layer reflectivity is inversely proportional to the depth. It results in a low emissivity and the attenuated Tb. The RMSE for the *in situ* simulation is 5.2, but it is based on a single observation of *in situ* stratigraphy during P1. In P2, *SodRad* experiences a significant Tb drop of about 20 K due to new snow arrival, seen as precipitation in mid-November 2010. The coupled simulation Tb did not show a Tb decrease like the *SodRad* Tb, while the *in situ* Tb did decrease slightly. This is reflected in the RMSE score of 11.9 and 15.2 K for the *in situ* and coupled cases. In P3, defined as "the steady snow accumulation period," the best comparison statistics are achieved with 6.3 K in the coupled case when excluding high peaks indicated by the dotted blue circles. The high peaks correspond to the moments when the coupled simulations have higher liquid water content and *SodRad* did not see the wetness. However, it is noted that the number of *SodRad* peaks at the same time as the blue dots is much smaller than high Tbs from the coupled simulations. The differences of coupled and *in situ* cases versus *SodRad* are identified by ΔC and Δi, whose values are ~80 and ~12 K, respectively. The high Tb discrepancies, ΔC (blue circles), can also be attributed to the 3 h observation interval of *SodRad* measurements. At the end of the snow accumulation period, (P3), the snowpack metamorphoses very fast when the temperature reaches the melting point. Finally, P4, defined as "the melting season" shows large jumps in *SodRad* Tbs and both simulations. Again, slight differences in the timing of the peaks between simulations and *SodRad* observations lead to the worst comparison statistics, with 33.7 and 37.9 RMSE for the *in situ* and coupled cases, respectively. The four temporal divisions of the snow season

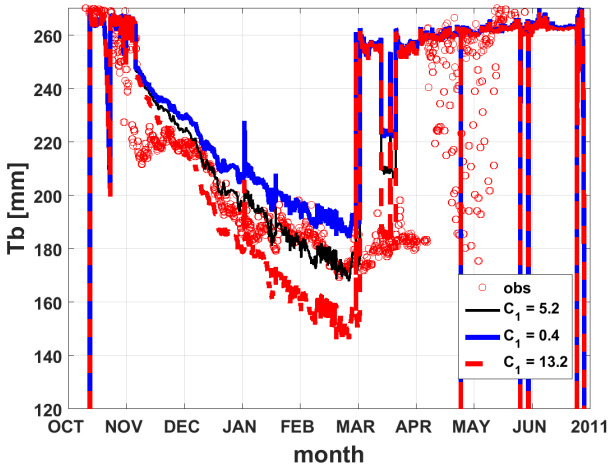


Fig. 11. MEMLS Tb sensitivity with varying grain growth adjustment factor, C_1 of 0.4, 5.2, and 13.2 compared with *SodRad* Tb. The snow model is set up with an initial snow grain size of 1.0 mm for three RTMs.

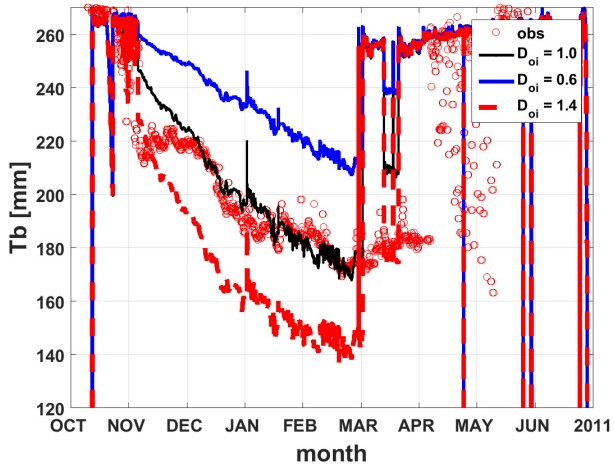


Fig. 12. MEMLS Tb sensitivity with varying initial snow grain sizes, D_{oi} of 1.0, 0.6, and 1.4 mm compared with *SodRad* Tb. The snow model is set up with the same snow grain growth rate of 1.3 mm/h for all three RTMs, equally applied to Fig. 11.

accommodate better physical explanations of how microwave signatures are related to the snowpack evolution. It may be advisable to apply such divisions to SWE retrieval algorithms to reduce the error caused by different behavior during melt, accumulation, and refreeze. Thus, the selective application of the RTM framework driven by the snow physics model (or by *in situ* or available snowpit measurements) would improve SWE retrieval performances based on the microwave volume scattering approach.

C. Sensitivity to Grain Growth Rate and Initial Grain Size

Fig. 11 shows setting factor $C_1 = 5.2$ in (3) properly fits the simulated grain size evolution with the observed snow grain size. With smaller or larger factors, snow grain sizes are underestimated/overestimated, leading to overestimated/underestimated Tbs, respectively. Fig. 12 shows the contributions to Tb of initial snow grain sizes of 1.0, 0.6, and 1.4 mm. It also confirms that for this type of grain-growth-based snow physics model, the initial value of the snow grain size is the key to accurately simulating Tb during the snow season. The coupled case RTM simulation performance

This article has been accepted for inclusion in a future issue of this journal. Content is final as presented, with the exception of pagination.

depends on the determination of the initial snow grain size and the growth rate during the evolution of the snowpack.

V. Conclusion

RTMs relate the physical state of snowpack with the observed microwave Tbs [10], [12]–[15]. This study compares the performance of three well-known RTMs at 36.5 GHz in controlled sensitivity experiments and when combined with a snow physics model to reproduce the observed Tb of a snowpack. The following are point-by-point findings from this article and recommendations for future RTM experiments, and ground-based Tb observations.

1) Scaling factors on the effective snow grain size are required to match the Tb predictions from the three RTMs. The scaling factors, $\alpha = 1.8$, $\beta = 1.0$, and $\gamma = 0.4$ are valid for small grain sizes less than 1 mm within the Rayleigh scattering [34] zone for frequencies at or below 36.5 GHz [23].
2) For larger grain sizes outside the Rayleigh scattering zone, HUT, in general, predicts higher Tb responses than MEMLS. This is because HUT has assumed an empirical power law of extinction coefficients κ_e on the grain size a: $\kappa_e \propto a^{2.0}$. This power coefficient is lower than what MEMLS predicts at ∼2.5. Thus, MEMLS leads to a steeper decrease in Tb with respect to grain size without the logarithmic scaling of the grain size. On the other hand, the DMRT-QMS, based on a physical scattering model, predicts a power coefficient that varies with frequency and the stickiness parameter.
3) HUT predicts the largest extinction coefficients and the highest Tbs for similar grain sizes compared with MEMLS and DMRT-QMS. This may seem counterintuitive, but it is due to the strong forward scattering assumed in HUT, where 96% of power is being scattered forward.
4) The combined snow physics and RTM simulations [9], [27], [28] utilizing the NoSREx data suggest that the *initial snow grain size* and the *grain size evolution curve* are effective in simulating Tb against the observed Tb *during the entire snow year*. Prior knowledge of the evolution of snow grain sizes would benefit RTM simulations in the coupled case. Also, this article shows the potential of the joint snow-physics and RTM to reproduce the observed Tb in a continuous time series, which can serve as foundational work for an optimization process to retrieve snow physical properties from space.
5) The *in situ* driven Tb performs with an RMSE of 21.0 K compared to 24.7 K by the coupled case Tb against the observed *SodRad* Tb. The difference of 3.7-K RMSE between *in situ* and coupled cases is attributed to the uncertainty associated with a snow physics model when driven by the external weather forcing. However, after isolating the snow accumulation period and excluding snowmelt events, much improved 12.2- and 6.3-K RMSEs are achieved during the water year 2011 from *in situ* and coupled simulations, respectively.
6) As shown in Fig. 10, when the entire snow year is divided into four periods, the best performance occurs during the snow accumulation period P3 with 6.3-K RMSE using the HUT RTM. Performances during the other three periods are affected by: surface melt during P1, continuous snowfall during P2, and diurnal melt in P4. These individual explanations allow a better understanding of the RMSE during each period.
7) The peaks and fluctuations [35] of Tbs due to the melt-refreeze processes are demonstrated in both the coupled-RTM simulations and the *SodRad* observations at NoSREx. The simulation results are more sensitive to the presence of liquid water than the *SodRad* observations (see ΔC and Δi in Fig. 10), possibly attributed to the immediate percolation of meltwater in the snow physics model. The timing of liquid water presence can be different between model simulation and *SodRad* observation because the coupled simulation runs hourly and the 3-h interval of *SodRad* observations might be too sparse to follow fast changes in snow wetness.

Some RTMs (such as the DMRT-QMS) already include active microwave parameters, such as backscattering coefficients. Thus, combining passive RTM with active RTM will facilitate the development of a more robust retrieval algorithm for terrestrial snow.

Acknowledgment

The authors would like to thank the following colleagues for sharing the microwave forward models of the snowpack. This includes Dr. C. Mätzler from the University of Bern, Bern, Switzerland, for MEMLS, Dr. J. Lemmetyinen from the Finnish Meteorological Institute for HUT, and Dr. L. Tsang from the University of Michigan, Ann Arbor, MI, USA, for DMRT-QMS. They would also like to thank the European Space Agency for the NoSREx 2009–2012 data set.

References

[1] A. H. Strahler, C. E. Woodcock, and J. A. Smith, "On the nature of models in remote sensing," *Remote Sens. Environ.*, vol. 20, pp. 121–139, Oct. 1986.
[2] R. Saunders, M. Matricardi, and P. Brunel, "An improved fast radiative transfer model for assimilation of satellite radiance observations," *Quart. J. Roy. Meteorol. Soc.*, vol. 125, no. 556, pp. 1407–1425, 1999.
[3] M. Weiss *et al.*, "Coupling canopy functioning and radiative transfer models for remote sensing data assimilation," *Agricult. Forest Meteorol.*, vol. 108, pp. 113–128, Jun. 2001.
[4] R. E. Kelly, A. T. Chang, L. Tsang, and J. L. Foster, "A prototype AMSR-E global snow area and snow depth algorithm," *IEEE Trans. Geosci. Remote Sens.*, vol. 41, no. 2, pp. 230–242, Feb. 2003.
[5] P. Gloersen and F. Barath, "A scanning multichannel microwave radiometer for Nimbus-G and Seasat-A," *IEEE J. Ocean. Eng.*, vol. OE-2, no. 2, pp. 172–178, Apr. 1977.
[6] M. Tiuri, A. Sihvola, E. Nyfors, and M. T. Hallikaiken, "The complex dielectric constant of snow at microwave frequencies," *IEEE J. Ocean. Eng.*, vol. OE-9, no. 5, pp. 377–382, Dec. 1984.
[7] M. T. Hallikainen, F. Ulaby, and M. Abdelrazik, "Dielectric properties of snow in the 3 to 37 GHz range," *IEEE Trans. Antennas Propag.*, vol. AP-34, no. 11, pp. 1329–1340, Nov. 1986.
[8] M. T. Hallikainen, F. T. Ulaby, and T. E. Van Deventer, "Extinction behavior of dry snow in the 18-to 90-GHz range," *IEEE Trans. Geosci. Remote Sens.*, vol. GRS-25, no. 6, pp. 737–745, Nov. 1987.

This article has been accepted for inclusion in a future issue of this journal. Content is final as presented, with the exception of pagination.

[9] A. Langlois, A. Royer, C. Derksen, B. Montpetit, F. Dupont, and K. Goïta, "Coupling the snow thermodynamic model SNOWPACK with the microwave emission model of layered snowpacks for subarctic and arctic snow water equivalent retrievals," *Water Resour. Res.*, vol. 48, no. 12, 2012, Art. no. W12524. doi: 10.1029/2012WR012133.

[10] W. H. Stiles, F. T. Ulaby, and A. Rango, "Microwave measurements of snowpack properties," *Hydrol. Res.*, vol. 12, no. 3, pp. 143–166, 1981.

[11] J. L. Foster, D. K. Hall, and A. T. C. Chang, "Remote sensing of snow," *EOS, Trans. Amer. Geophys. Union*, vol. 68, no. 32, pp. 682–684, 1987.

[12] A. Wiesmann and C. Mätzler, "Microwave emission model of layered snowpacks," *Remote Sens. Environ.*, vol. 70, pp. 307–316, Dec. 1999.

[13] C. Mätzler and A. Wiesmann, "Extension of the microwave emission model of layered snowpacks to coarse-grained snow," *Remote Sens. Environ.*, vol. 70, no. 3, pp. 317–325, 1999.

[14] L. Tsang, C.-T. Chen, A. T. C. Chang, J. Guo, and K.-H. Ding, "Dense media radiative transfer theory based on quasicrystalline approximation with applications to passive microwave remote sensing of snow," *Radio Sci.*, vol. 35, no. 3, pp. 731–749, May/Jun. 2000.

[15] J. T. Pulliainen, J. Grandell, and M. T. Hallikainen, "HUT snow emission model and its applicability to snow water equivalent retrieval," *IEEE Trans. Geosci. Remote Sens.*, vol. 37, no. 3, pp. 1378–1390, May 1999.

[16] M. Tedesco and E. J. Kim, "Intercomparison of electromagnetic models for passive microwave remote sensing of snow," *IEEE Trans. Geosci. Remote Sens.*, vol. 44, no. 10, pp. 2654–2666, Oct. 2006.

[17] R. Jordan, "A one-dimensional temperature model for a snow cover: Technical documentation for SNTHERM. 89," U.S. Army Cold Reg. Res. Eng. Lab., Hanover, NH, USA, Spec. Rep. 91-16, 1991, p. 5.

[18] U. Inan, and A. Inan, *Electromagnetic Waves*. Upper Saddle River, NJ, USA: Prentice-Hall, 2000, p. 141.

[19] H. Löwe and G. Picard, "Microwave scattering coefficient of snow in MEMLS and DMRT-ML revisited: The relevance of sticky hard spheres and tomography-based estimates of stickiness," *Cryosphere*, vol. 9, no. 6, pp. 2101–2117, 2015. doi: 10.5194/tc-9-2101.

[20] A. Royer *et al.*, "Comparison of commonly-used microwave radiative transfer models for snow remote sensing," *Remote Sens. Environ.*, vol. 190, pp. 247–259, Mar. 2017. doi: 10.1016/j.rse.2016.12.020.

[21] G. Picard *et al.*, "Simulation of the microwave emission of multi-layered snowpacks using the Dense Media Radiative transfer theory: The DMRT-ML model," *Geosci. Model Develop.*, vol. 6, no. 4, pp. 1061–1078, 2013.

[22] J. Pan *et al.*, "Differences between the HUT snow emission model and MEMLS and their effects on brightness temperature simulation," *IEEE Trans. Geosci. Remote Sens.*, vol. 54, no. 4, pp. 2001–2019, Apr. 2016. doi: 10.1109/TGRS.2015.2493505.

[23] M. Sandells, R. Essery, N. Rutter, L. Wake, L. Leppänen, and J. Lemmetyinen, "Microstructure representation of snow in coupled snowpack and microwave emission models," *Cryosphere*, vol. 11, no. 1, pp. 229–246, 2017. doi: 10.5194/tc-11-229-2017.

[24] C. Maätzler, "Relation between grain-size and correlation length of snow," *J. Glaciol.*, vol. 48, no. 162, pp. 461–466, 2002.

[25] B. Montpetit, A. Royer, A. Roy, A. Langlois, and C. Derksen, "Snow microwave emission modeling of ice lenses within a snowpack using the microwave emission model for layered snowpacks," *IEEE Trans. Geosci. Remote Sens.*, vol. 51, no. 9, pp. 4705–4717, Sep. 2013.

[26] M. Durand, E. J. Kim, and S. A. Margulis, "Quantifying uncertainty in modeling snow microwave radiance for a mountain snowpack at the point-scale, including stratigraphic effects," *IEEE Trans. Geosci. Remote Sens.*, vol. 46, no. 6, pp. 1753–1767, Jun. 2008.

[27] A. Wiesmann, C. Fierz, and C. Mätzler, "Simulation of microwave emission from physically modeled snowpacks," *Ann. Glaciol.*, vol. 31, no. 1, pp. 397–405, 2000.

[28] D.-H. Kang and A. P. Barros, "Observing system simulation of snow microwave emissions over data sparse regions—Part II: Multilayer physics," *IEEE Trans. Geosci. Remote Sens.*, vol. 50, no. 5, pp. 1806–1820, May 2012.

[29] A. Kontu, J. Lemmetyinen, J. Vehviläinen, L. Leppänen, and J. Pulliainen, "Coupling SNOWPACK-modeled grain size parameters with the HUT snow emission model," *Remote Sens. Environ.*, vol. 194, pp. 33–47, Jun. 2017.

[30] J. Lemmetyinen, J. Pulliainen, A. Rees, A. Kontu, Y. Qiu, and C. Derksen, "Multiple-layer adaptation of HUT snow emission model: Comparison with experimental data," *IEEE Trans. Geosci. Remote Sens.*, vol. 48, no. 7, pp. 2781–2794, Jul. 2010.

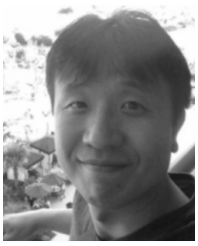
[31] A. Kontu and J. Pulliainen, "Simulation of spaceborne microwave radiometer measurements of snow cover using *in situ* data and brightness temperature modeling," *IEEE Trans. Geosci. Remote Sens.*, vol. 48, no. 3, pp. 1031–1044, Mar. 2010.

[32] J. Lemmetyinen *et al.*, "Nordic snow radar experiment," *Geosci. Instrum. Methods Data Syst.*, vol. 5, pp. 403–415, Sep. 2016.

[33] M. Lehning, P. Bartelt, B. Brown, C. Fierz, and P. Satyawali, "A physical SNOWPACK model for the Swiss avalanche warning: Part II. Snow microstructure," *Cold Regions Sci. Technol.*, vol. 35, pp. 147–167, Nov. 2002.

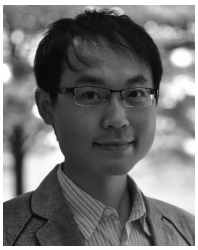
[34] A. T. Young, "Rayleigh scattering," *Appl. Opt.*, vol. 20, no. 4, pp. 533–535, 1981.

[35] M. R. Anderson, "The onset of spring melt in first-year ice regions of the Arctic as determined from scanning multichannel microwave radiometer data for 1979 and 1980," *J. Geophys. Res.*, vol. 92, no. C12, pp. 13153–13163, 1987.



Do Hyuk Kang (M'19) received the B.A. degree in geography from Seoul National University, Seoul, South Korea, and the M.S. and Ph.D. degrees from Colorado State University, Ft. Collins, CO, USA, and Duke University, Durham, NC, USA, respectively.

He is currently an Assistant Research Scientist with the Earth System Science Interdisciplinary Center, University of Maryland, College Park, MD, USA, and the NASA Goddard Space Flight Center, Greenbelt, MD, USA. He has authored more than eight peer-reviewed publications on snow microwave remote sensing and snow hydrological processes. His primary research lies on a coupled model approach between a microwave forward model and a snow hydrology model to improve retrieval algorithms based on microwave signatures of the snowpack.



Shurun Tan (S'14–M'17) received the B.Eng. and M.Eng. degrees in electrical engineering from Southeast University, Nanjing, China, in 2009 and 2012, respectively, and the Ph.D. degree in electrical engineering from the University of Michigan, Ann Arbor, MI, USA, in 2016.

In January 2019, he joined the Zhejiang University/University of Illinois at Urbana–Champaign Institute, Haining, China, as an Assistant Professor. From December 2010 to November 2011, he was a Visiting Student with the Department of Electrical and Computer Engineering, the University of Houston, Houston, TX, USA. From September 2012 to December 2014, he was a Ph.D. candidate with the Department of Electrical Engineering, University of Washington, Seattle, WA, USA. From January 2015 to December 2018, he was affiliated with the Radiation Laboratory, Department of Electrical Engineering and Computer Science, University of Michigan, Ann Arbor, first as a Ph.D. candidate, and then as a Post-Doctoral Research Fellow since January 2017. His research interests include electromagnetic theory, computational and applied electromagnetics, wave propagation and scattering in random media and periodic structures, radar and radiometric geophysical remote sensing of terrestrial snow, polar ice sheet, sea ice, ocean, and vegetated land surfaces, photonic crystals and metamaterials, topological acoustics and photonics, electromagnetic compatibility and signal integrity, and multi-scale and multiphysics analysis.



Edward Kim (S'90–M'99–SM'05) received the S.B. and S.M. degrees in electrical engineering from the Massachusetts Institute of Technology, Cambridge, MA, USA, and a joint Ph.D. degree from the Department of Electrical Engineering and Atmospheric Sciences, University of Michigan, Ann Arbor, MI, USA, in 1998.

Since 1999, he has been with NASA's Goddard Space Flight Center, Greenbelt, MD, USA, where he has been involved in remote sensing of snow, soil moisture, frozen soil, and the atmosphere as well as satellite mission development. His research interests include instrument development, field campaigns, electromagnetic modeling, retrieval algorithms, and calibration.

Dr. Kim served as the Project Scientist for NASA's 2017 SnowEx campaign and continues to work with the snow remote sensing community toward a snow satellite mission. He also serves as NASA's Instrument Scientist for the ATMS microwave sounder on the S-NPP and JPSS satellites.